RESERVE THIS SPACE

Circumstellar Chemistry

and Dust From Dead Stars in Meteorites

Katharina Lodders

Department of Earth and Planetary Sciences and McDonnell Center for the Space Sciences, Washington University, Saint Louis, MO 63130

This chapter briefly introduces the chemistry in circumstellar envelopes (CSE) around old, mass-losing stars. The focus is on stars with initial masses of one to eight solar masses that evolve into red giant stars with a few hundred times the solar radius, and which develop circumstellar shells several hundred times their stellar radii. The chemistry in the innermost circumstellar shell adjacent to the photosphere is dominated by thermochemistry, whereas photochemistry driven by interstellar UV radiation dominates in the outer shell. The conditions in the CSE allow mineral condensation within a few stellar radii, and these grains are important sources of interstellar dust. Micron-sized dust grains that formed in the CSE of red giant stars have been isolated from certain meteorites and their elemental and isotopic chemistry provides detailed insights into nucleosynthesis processes and dust formation conditions of their parent stars, which died before the solar system was born 4.56 Ga ago.

RESERVE THIS SPACE

Giant Star Evolution and the Circumstellar Environment

The evolution of low and intermediate mass stars to mass-losing giant stars and the associated processes creating and operating in circumstellar environments are reviewed in (*1-10*). The following summary serves to place the circumstellar chemistry into context. Table I gives some symbols and values frequently used in astronomy, and Table II some properties of the Sun and giant stars. Most dwarf stars near the Sun have elemental abundances similar to those in the solar photosphere, which are generally used as a reference composition (*11*). Low-mass dwarf stars like the sun burn H to He mainly through the proton-proton chain, but, with increasing mass, the CNO cycle, in which nitrogen is a by-product, becomes more important. As long as H-burning occurs in the core, elemental abundances on the stellar exterior remain practically unchanged. Dwarf stars with masses of ~1 to 8 solar masses ($M_\odot$) evolve into giant stars after hydrogen fuel is exhausted in their cores (~10^{10} years for the Sun). The first changes in surface composition appear in the red giant (RG) stage, when the N produced in the CNO cycle is mixed up from the stellar interior (the so-called first dredge-up). These stars then burn He to C and O in their cores.

After He is exhausted in their cores, stars alternately burn H and He in shells surrounding the electron-degenerate carbon-oxygen core. Stars > 4 $M_\odot$ can experience a second dredge up of CNO cycle products during this stage. The H- and He-shell-burning stars are located on the asymptotic branch moving off the main sequence defined by dwarf stars in the Hertzsprung-Russell diagram; hence, they are called asymptotic giant branch (AGB) stars. The AGB stars experience multiple thermal pulses when He-shell burning ignites every ~10,000 years. These thermal pulses are responsible for the "3rd-dredge-up" episodes, which bring ^{12}C, produced by previous He-shell burning, along with s-process elements up to the stellar surface (7). Many isotopes of elements heavier than Fe (e.g., Y, Zr, Sr, Ba) are primarily produced by *slow* neutron capture nucleosynthesis in AGB stars and are therefore referred to as "s-process elements".

Table I. Useful Astronomical Quantities

Quantity	*Symbol*	*Unit Value*
Mass of Sun	$M_\odot$	1.99×10^{30} kg
Radius of Sun	$R_\odot$	6.96×10^{8} m
Astronomical Unit (Earth-Sun distance)	AU	1.50×10^{11} m
Luminosity of Sun	$L_\odot$	3.83×10^{26} W
Mass-loss rate, dM/dt	$M_\odot$/yr	6.30×10^{22} kg/s
Stefan-Boltzmann constant	σ	5.67×10^{-8} W/(m^{2}K^4)
Gravitational constant	G	6.67×10^{-11} m^3/(kg s^2)

Table II. Properties of the Sun and Cool AGB Stars

Property	*Sun*	*M*	*S*	*C*
Effective Temp. (K)	5780	2600-3300	2300-3100	2200-3000
Radius, $R_\odot$	≡1	160 – 370	270 – 530	400 – 560
Luminosity, $L_\odot$	≡1	100 – 10^4	2000 – 10^4	2000 – 10^4
A(H)	≡ 12	≡ 12	≡ 12	≡ 12
A(C)	8.39	8.52	8.55	8.75
A(N)	7.83	8.28	8.77	7.78
A(O)	8.69	8.86	8.75	8.70
A(Fe)	7.45	7.37	7.36	7.36
C/O (atomic)	0.50	0.45	1.00	1.14
s-process elements	≡ 1	~ 1-5	~5 – 10	~ 5 - 100
dM/dt, $M_\odot$/yr	10^{-14}	10^{-8} – 10^{-4}	10^{-8} – 10^{-6}	10^{-8} – 10^{-4}
Dust seen in CSE	None	silicates, oxides	silicates SiC (rare)	SiC, carbon

NOTE: Abundances A(i) are given in the standard astronomical notation on a logarithmic scale where the number of H atoms is defined (≡) as log N(H) = 12. For M, S, and C stars, average or characteristic values are listed.

SOURCE: Modified from (*34*)

The increased energy output from He-core burning, and subsequent H- and He-shell burning literally turns dwarfs into giants: RG stars have radii of ~10-50 $R_\odot$ and AGB stars ~100-600 $R_\odot$ (*12*) (the Sun-Earth distance is ~215 $R_\odot$). The effective temperatures (i.e. the temperature equivalent to an ideal blackbody) of giant stars (~2000-3500 K) are lower than those of dwarf stars of similar mass. Thus, giant stars emit most of their radiation at red wavelengths. Red giant stars have luminosities ($L = 4\pi\sigma R^2 T_{eff}^4$) up to 10,000 times greater than the sun.

The atmospheres of low-mass dwarf stars are relatively tightly bound by gravitation, and mass loss from their outer atmospheres is very low; e.g., the Sun loses ~10^{-14} $M_\odot$/yr. For stars of the same mass, the surface gravity ($g = GM/R^2$) decreases with increasing radius. For example, the Sun's gravity (in cm/s^2 and logarithmic form as preferred by astronomers) is log g = 4.4, whereas a 1 $M_\odot$ AGB star with 215 $R_\odot$ has log g ~0.2. Then atmospheric pressure scale heights (H) are larger and required escape velocities are smaller. (The scale height is defined as $H = RT/\mu g$ where *R* is the gas constant and μ is the mean molecular weight). Relatively small radial oscillations may become sufficient to levitate the outer atmosphere enough to allow it to escape. The matter lost from the expanded atmospheres creates more or less spherical

circumstellar shells, also called circumstellar envelopes (CSE). Observed mass-loss rates in RG stars are ~10^{-7} $M_{\odot}$/yr or less, and range from 10^{-7} to 10^{-4} $M_{\odot}$/yr in AGB stars (*13-15*). Annual mass-loss for RG stars can be estimated from Reimers' formula $dM/dt = 4\times10^{-13}\eta LR/M$, where η is a constant between ~1/3 to ~3, and L, R, and M are in solar units. However, mass-loss rates for AGB stars are typically underestimated by this equation.

The higher mass-loss rates in AGB stars are caused by stellar pulsation and grain condensation in their CSE (*16-20*). Many AGB stars are radially-pulsating variable stars with periodic changes in luminosity. They are either irregular (Lb) or semi-regular (SR) variables with periods of 50 – 300 days, or are Mira-type variables with regular periods of 100 – 1000 days (*21*). A periodic variation in stellar radii implies that mass can escape the star on regular cycles. Observed mass-loss rates and expansion velocities tend to correlate well with variability periods (*14*). The atmospheric pulsations produce shock waves that propagate into the CSE where they dissipate (*22*). Thus, the temperature, density, and, likely, the chemistry in the CSE are dynamically coupled to the stellar atmosphere with timescales similar to those of the luminosity variability periods. Detailed models of stellar atmospheres and circumstellar shells take these time-dependent variations into account (*15,22-25*).

Figure 1 is an idealized sketch of a CSE around an AGB star to show the variations of temperature and density as a function of radial distance. A typical AGB star has a stellar radius (R_*) ~3.5×10^{15} cm ~500 $R_{\odot}$. Near the photosphere, the T and P structure is determined by hydrostatic equilibrium of the star (e.g., *25-28*). In the transition zone, T and P drop due to adiabatic expansion and, to some extent, radiative cooling. Within $\leq$5 stellar radii, conditions in the CSE become favorable for dust condensation. Dust formation speeds up the loss of the stellar atmosphere through dust-driven winds (*8,16-20*). Dust grains are accelerated by radiation pressure, and, through momentum transfer, the dust drags the surrounding gas outwards. This leads to terminal expansion velocities ranging from 5-25 km/s, with typical values around 10-15 km/s (*13-15*). The density (ρ) in the CSE is related to the mass-loss rate as $dM/dt = 4\pi R^2\rho(R)v_{exp}(R)$, and temperatures follow $T(R) = T_o(R_o/R)^{\alpha}$, where α = 0.6–0.8 is a measure of the heating and cooling processes in the outflowing gas. The outer limit of the CSE is given by the duration of mass-loss, e.g., for v_{exp}= 10 km/s, the CSE grows by ~2 AU per year. Observed mass-loss rates correlate with expansion velocities, and dM/dt seems to increase with stellar luminosity as well as inverse effective temperature (*14,15*), which is consistent with the idea that radiation pressure acting on grains is driving the mass-loss.

On longer timescales, such as the duration of the AGB stage, the mass-loss from giant stars is more or less continuous, but there is evidence for episodes of increased mass-loss for which the reasons are not entirely clear. Some objects show clumpiness in their CSEs, and several stars have detached shells or

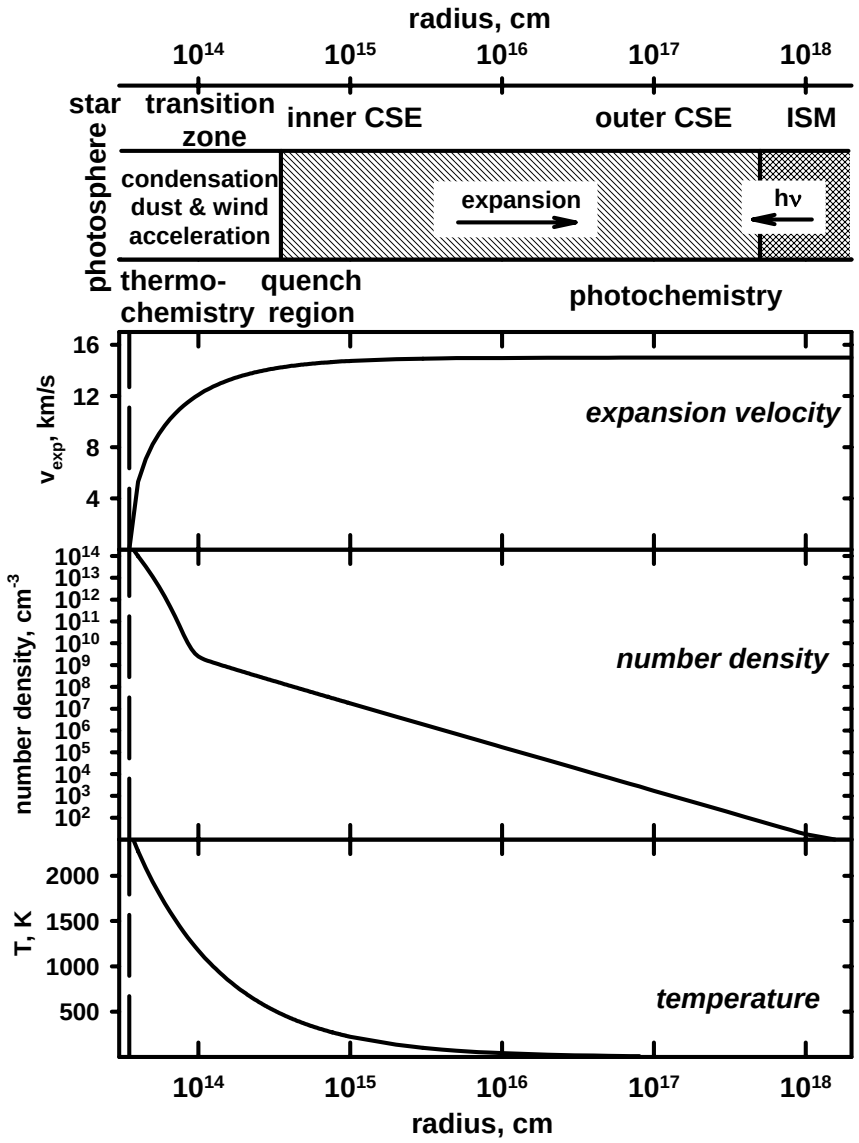

Figure 1. Approximate conditions in a circumstellar envelope around an AGB star of ~500 $R_\odot$ (3.5×10^{13} cm) and 1$M_\odot$

multiple circumstellar shells expanding at different speeds, indicating different ejection times of material. This may be related to the thermal pulses caused by

ignition of He-shell burning (*14*,*29*). Some objects with large mass-loss rates (~10^{-4} $M_{\odot}$/yr) developed very thick circumstellar shells that obscure detection of the central stars at optical wavelengths. Several enshrouded objects were discovered first by infrared emission from their circumstellar shells (e.g., *30*).

Dust-driven winds are thought to be the major cause for the complete loss of an AGB star's H- and He-rich atmosphere. Loss of the stellar envelope to the CSE limits the duration of the AGB stage to ~10^5 to 10^6 years. The last material leaves an AGB star in a fast superwind that shocks and ionizes the older, chemically processed CSE ejecta, which then appears as a so-called planetary nebula that surrounds a white dwarf – the remnant C-O-rich stellar core (*31*).

Elemental Abundances and Gas Chemistry

The major elements whose abundances are affected by nucleosynthesis in giant stars are C, N, and O (when compared to solar abundances). This affects the molecular speciation of many other elements in cool stellar atmospheres and their CSEs because C and O play a key role in determining the overall oxidation state. Stellar spectroscopy uses the changing molecular chemistry caused by an increase in C to classify cool RG stars into O-rich and C-rich stars. The carbon to oxygen (C/O) ratio in the sun is about 0.5. Figure 2 illustrates the calculated changes in gas chemistry for a few elements when the C/O ratio is increased by adding C to an otherwise solar composition gas at T and P conditions roughly representative of photospheric regions (see *32*-*35*).

Elemental Abundance Classification of Stars: M, S, and C Stars

Cool O-rich giant stars with C/O < 1 (M stars) have elemental abundances comparable to those of the Sun, and the gas molecules identified in their photospheric spectra (e.g., CO, H_2O, TiO, VO, ZrO) are similar to those expected to form in a gas with solar elemental composition based upon thermochemical computations (Figure 2). The major C- and O-bearing gases in a solar gas are CO and H_2O. Essentially all C is locked up in the very stable CO molecule. Oxygen is twice as abundant, and most O is evenly distributed between CO and H_2O gas. The metal oxide abundances are limited by the total metal abundances, which are typically much less than that of oxygen, and metal distribution into other gases such as sulfides must be considered as well. The C/O ratio is not changed by much in cool red giant stars, and their gas chemistry is quite similar to that of a solar gas. Although the N abundances in red giant stars are higher due to the first dredge-up, an increase in N abundance does not

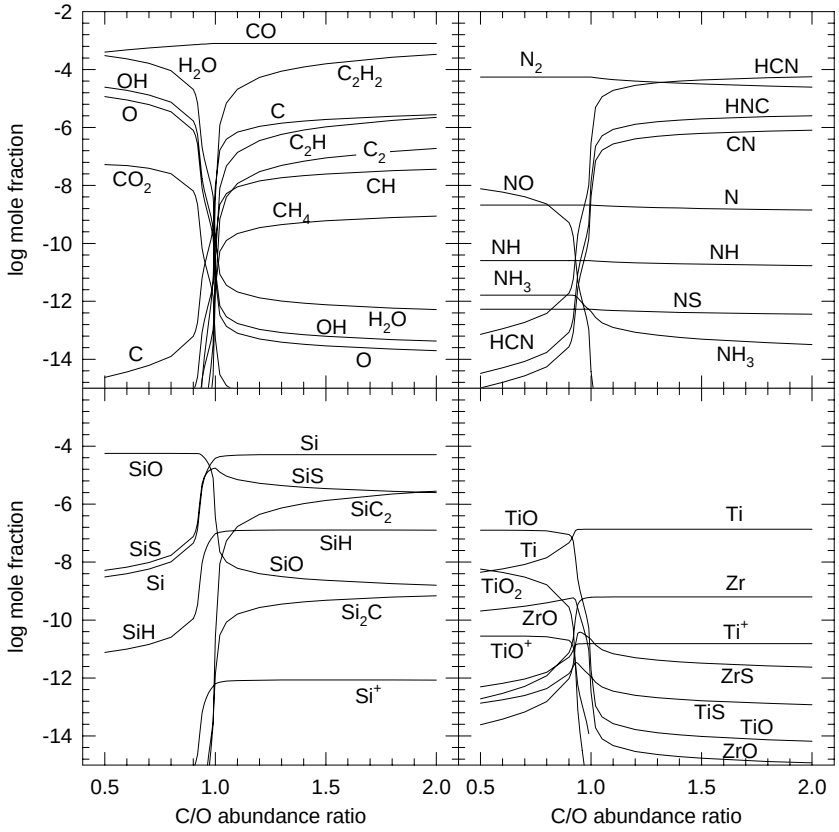

Figure 2. Thermochemical equilibrium abundances (mole fractions) as a function of C/O ratio at 2000 K and $P_{tot}=10^{-5}$ bar. Only a few gases are shown to illustrate trends.

affect the chemistry of other elements very much because nitrogen is mainly present as N_2 and atomic N.

The C/O ratio increases in the outer atmosphere during the AGB stage by continuous dredge-up of C from the stellar interior. Stars with C/O near unity are called S stars. They still show CO and oxides in their spectra, but, because more O is in CO, the abundances of other oxides drop. The abundances of neutral and ionized atoms and sulfides are not affected much by an increase in the C/O ratio. One characteristic of S stars is that they show stronger ZrO absorption bands than observed in M stars with comparable temperatures (*36*). This appears to be at odds with the expected trend of decreasing oxide abundances with increasing C/O ratio (Figure 2). However, Zr is produced by s-

process nucleosynthesis and is dredged up to the surface of these AGB stars like many other s-process elements, which are more abundant in S stars than in M stars (*36*,*37*). The presence of radioactive Tc, which has a relatively short half-life of 2×10^5 years and therefore must be made in the star where it is observed, is proof that nucleosynthesis is indeed responsible for the observed s-process element enrichments.

Stars with C/O > 1 are called carbon (C) stars. It was quickly recognized after their discovery in the 1860s that the presence of molecules such as C_2 requires reducing atmospheres (see (*34*) for a historical review). If C is more abundant than O, essentially all O is locked up in CO, and water is no longer a major gas. The C not tied up in CO is distributed among molecules such as C_2H_2, CH, C_2H, C_2, CN, HCN, and HNC (Figure 2). The metals that form oxides in M and S stars are instead present as atoms and sulfides in C stars, and carbide gases such as SiC_2 and Si_2C appear (*32*-*35*).

Some cool giants are heavily enshrouded by their CSE and are mainly detectable in the infrared. Oxygen-rich AGB stars with strong infrared brightness and OH maser emission are so-called OH/IR stars. The closest C-rich AGB star with a thick CSE is IRC +10216 at a distance of 100-200 parsec (330-650 light years). Its CSE is a fruitful observation ground where most organic molecules observed in circumstellar shells were discovered (see Table III).

Table III. Molecules Detected in Circumstellar Shells

O & C rich shells	*O-rich shells*	*C-rich shells*
CO, H_2O, OH	CO_2	C_n (n=2-5), CH_4, C_2H_2, C_2H_4, C_nH (n=2-8), C_nH_2 (n=3,4,6), C_6H_6, C_3O, H_2CO, HCO^+, C_6H^-
HCN, HNC, CN, NH_3		C_3N, C_5N, HC_nN (n=2-5,7,911), CH_3CN, HC_2NC
CS, SiO, SiS, H_2S	SO, SO_2, OCS	C_2S, C_3S, SiH_4, SiC_n (n=1-4),$HSiC_2$, SiN, SiNC, SiCN, HCl, NaCl, NaCN, KCl, MgCN, MgNC, AlF, AlCl, AlNC

Circumstellar Envelope Chemistry

Photosphere and Inner CSE: Dust Condensation and Thermochemistry

This chemistry occurs in the transition zone (Figure 1), where stellar winds drive hot gas from the photosphere into the circumstellar environment. Dust

condensation also occurs relatively close to the photosphere in the cooling, expanding gas. Observations indicate that dust forms within 3-5 stellar radii of the central star (*38*,*39*). Several minerals become stable between 1000–2000 K. Figure 3 shows the types of condensates as a function of C/O ratio at a constant total pressure of 10^{-5} bar. The relative condensation sequence does not change much at different total pressures. Generally, condensation temperatures decrease with lower total pressures. The major point here is that the types of condensates change from refractory oxides, silicates, and metals at C/O< 1 to carbonaceous condensates such as graphite, carbides, and nitrides (such as AlN) at C/O>1 (e.g., *33*-*35*). The condensation temperatures decrease as C/O increases from 0.5 to 1 because CO consumes more O and less is available for oxide formation. Aside from O and C, the major condensate-forming elements are Si, Mg, and Fe. Their condensates should be the most abundant minerals, and M, S, and C stars should have different types of minerals in their CSEs.

The radiation from the central star heats the dust in the CSE to higher temperatures than the surrounding gas. This leads to thermal emission from the dust. The dust closer to the photosphere at 1500-1000 K emits in the near infrared (1-5 microns) and dust further out at 500 K emits at mid-infrared wavelengths (up to ~20 microns). Iron metal is infrared inactive and its predicted presence in CSEs is difficult to confirm. However, Mg-silicates, such as forsterite (Mg_2SiO_4, an olivine) and enstatite ($MgSiO_3$, a pyroxene), have been detected by IR spectroscopy in M star CSEs. Infrared studies show that amorphous and crystalline pyroxenes and olivines are present and are typically Mg-rich, with minor, varying amounts of Fe substituting for Mg (e.g., fayalite Fe_2SiO_4 and ferrosillite $FeSiO_3$) (*40*). Carbon stars contain SiC and carbon in their CSEs, and the 11.3 micron infrared emission feature of SiC is a well-known characteristic of C stars (*41*). Another expected major mineral condensing at ~1020 K is MgS, which may be responsible for the 30 micron emissions in some C stars (*42*). Dust from AGB stars is not only studied by astronomical observations but also in the laboratory because genuine stardust from AGB stars is found in meteorites (see below).

The spatial extent of the circumstellar environment and outflow conditions such as expansion velocities and stellar mass-loss rates can be probed using circumstellar line emissions in infrared to radio wavelengths for many molecules (e.g., CO, OH, H_2O, CN, HCN, CS, SiO, SiS) (*13*-*15*, *20*, *44*-*51*). The abundances of the molecules CO, C_2H_2, HCN, CS, SiO and SiS are thought to be established from equilibrium thermochemistry near the photosphere (Figure 2).

However, as temperatures and densities drop steeply in the circumstellar shell with increasing distance from the central star, reaction kinetics may no longer permit establishment of thermochemical equilibrium in the stellar outflow (*4*). Detailed and generally applicable discussions of the reaction

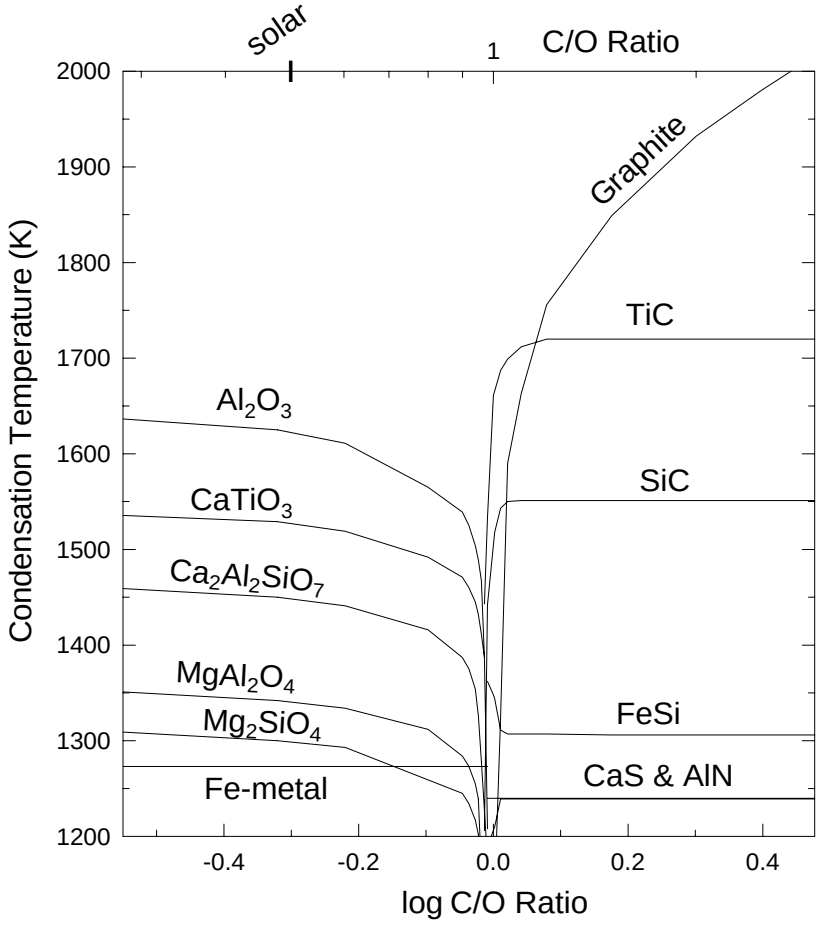

Figure 3. Major condensates and condensation temperatures as a function of C/O ratio at 10^{-5} bar total pressure. At C/O>1, MgS condenses at ~1020K.

kinetics relevant here can be found in (*52*,*53*). Let us follow a parcel of hot atmospheric gas traveling away from the photosphere and assume that a certain gas is produced or destroyed by some reaction in the CSE. As long as chemical reaction times (τ_{chem}), which are different for different gases, are shorter than residence times determined by the expansion velocity in the CSE (τ_{exp} (R) = H/v_{exp}), one should expect that the gas abundance can be modeled by thermochemical equilibrium. Fast reaction times are favored by high temperatures and high total pressures, so equilibrium conditions are best

realized in the photospheric and adjacent shell regions. At the quench distance R_Q, where $\tau_{exp}(R) = \tau_{chem}$, the abundance of our sample gas becomes "frozen in". At $R > R_Q$, the residence time of the gas parcel is shorter than the reaction time ($\tau_{chem} > \tau_{exp}$) required to reach reaction equilibrium at the given T and ρ conditions. As a rough guide, endothermic reactions with higher activation energies are quenched closer to the star than exothermic reactions, and reactions involving radicals are expected to operate at large distances from the star (*4*,*52*,*53*).

Chemical equilibrium abundances for many C-, N-, and O-bearing gases for T = 500-2500K and P = 10^{-7} - 1000 bars for a solar composition gas can be found in (*54*). Although these calculations were applied to brown dwarfs and giant planet atmospheres, the pressure conditions also include those appropriate for O-rich photospheres and their inner CSEs (10^{-4} – 10^{-7} bars).

The very stable molecules CO (observed) and N_2 (not observable) are the major C-, O-, and N-bearing gases throughout the entire CSE, as expected from thermochemical equilibrium. Under the low total pressures in the CSE, conversions of CO to CH_4 or N_2 to NH_3 as the major C- or N-bearing gases does not occur. Even if pressure conditions were favorable, these reactions would not reach equilibrium because they are kinetically inhibited (these conversions are quenched even in the much denser giant planet atmospheres (e.g., *54*). This does not mean that CH_4 or NH_3 should be absent from the CSE; it only means that their abundances are likely less than that expected from thermochemical equilibrium. In O-rich CSE, most oxygen is evenly distributed between CO and H_2O, but CO_2, produced by the rapid water gas reaction ($CO + H_2O = H_2 + CO_2$) is also an abundant gas (*54*) and has been observed.

Many investigations of circumstellar molecules have been done for C-rich CSE. Figure 4 shows observed abundance trends of several molecules as a function of radial distance in the thick CSE of the well-studied C star IRC+10216. The top shows gases whose abundances are determined by thermochemical equilibrium and quenching near the photosphere; the center panel shows molecules that seem to originate beyond ~ $10R_*$ (within the CSE), and the bottom panel shows some of the mainly photochemically-produced gases.

The CO/H_2 ratio remains constant throughout the CSE because CO is always the most thermochemically and kinetically stable O-bearing gas. CO is only destroyed by photodissociation in the outer CSE. One can assume that N_2, which is not observable, behaves similarly. Abundances of C_2H_2, HCN, CS, SiO (*50*) and SiS (*45*) are controlled by thermochemical equilibria near the photosphere (within ~1-3 R_*), which includes quenching of gas-phase reactions and control of gas abundances by condensate formation. These "parent" molecules are sources for the chemistry in the middle and outer CSE.

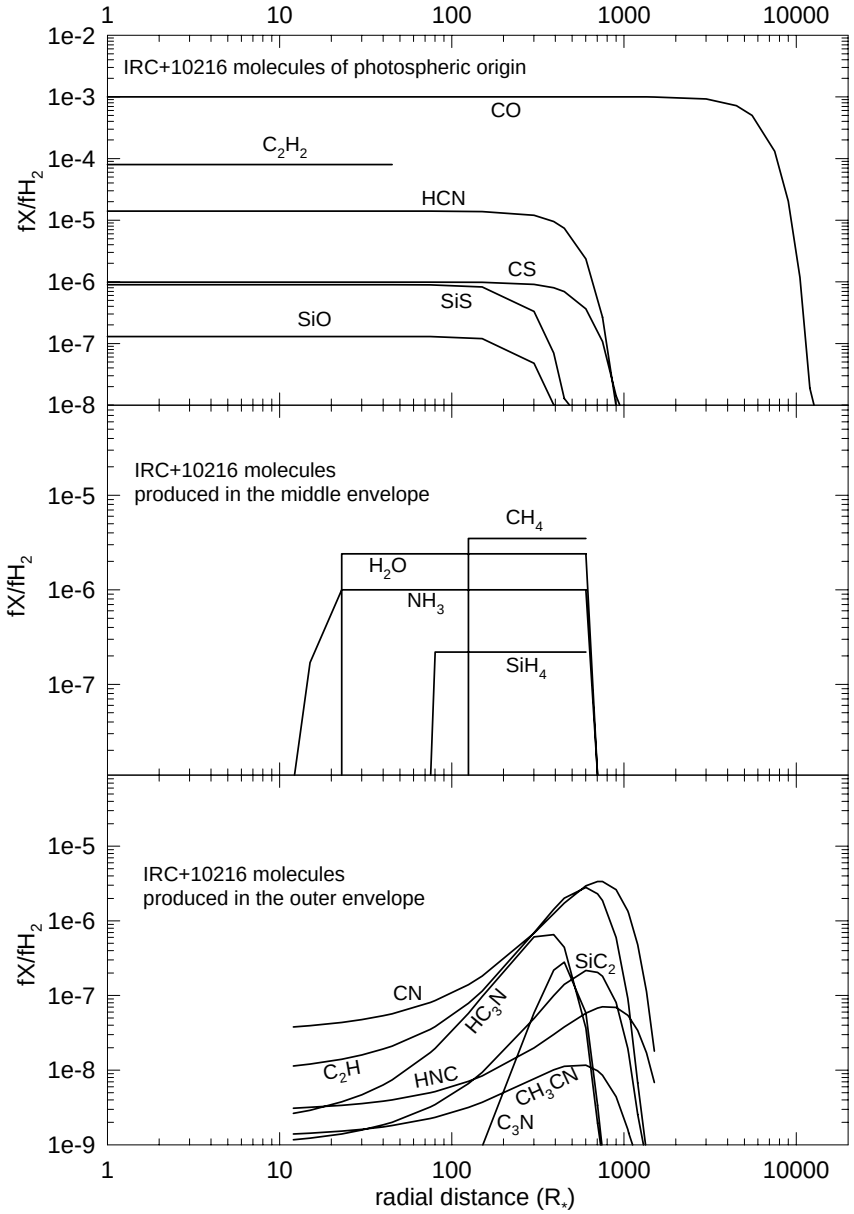

Figure 4. Abundance ratios (relative to hydrogen) of molecules and their emitting regionsas a function of radial distance (in stellar radii) in the C-rich CSE of IRC+10216. See text for references.

Middle Envelope Region: Reaction Kinetics and Dust-Gas Reactions

Around 10 R_*, abundances of CH_4 (*44*), NH_3 (*44,55,56*), H_2O (*56*), and SiH_4 (*44,55*) increase and remain until their likely photochemical destruction in the outer CSE. Their peak abundances are considerable, but do not exceed the maximum abundances of the photospheric molecules. They are, however, higher than expected from thermochemical equilibrium. The reaction pathways leading to the formation of CH_4, NH_3, H_2O, and SiH_4 are not clear, but grain-surface reactions are likely involved (44,52). The presence of dust may foster several types of reactions. Neutral molecule gas-phase reactions may proceed through grain surface catalyses. An argument against surface-catalyzed reactions is that CH_4, NH_3, H_2O, and SiH_4 abundances should begin to increase within the grain condensation region much closer to the star, but they do not. However, dust temperatures closer to the star could simply be too high to allow efficient gas adsorption, so that only the cooler dust further out may be catalytically active (*55*).

Another possible dust-driven reaction is parent molecule destruction by collisions with dust grains, e.g., H_2O + dust $\rightarrow$ OH + H + dust (more relevant to O-rich CSE) and HCN + dust $\rightarrow$ CN + H + dust. This may be a source for radicals to build new molecules through radical + neutral reactions (*17,52*). The parent molecule for NH_3 production is not well known. Abundant HCN could be one source in C-rich CSE. However, NH_3 has also been observed in O-rich CSE (*57*), which have very low HCN abundances. This would argue against a production mechanism involving HCN (see Figure 2 for HCN abundances in O- and C-rich photospheres).

The increase of SiH_4 (silane) is roughly correlated with the decrease in SiS and SiO abundances, but it seems unlikely that SiH_4 is produced directly from either SiO or SiS gas. Silane is only known to occur in C-rich CSE, whereas SiO and SiS are present in both C and O-rich CSEs. The depletion of SiO and SiS (as well as CS) is likely related to the continuing condensation of SiC and MgS. In that case, other Si-bearing gases should also become depleted but not produced. The detection of relatively large amounts of H_2O in the C-rich CSE of IRC+10216 is unexpected because essentially all O is bound in CO, which is not yet photodissociated at the distances where H_2O is observed (*56*). Overall, convincing models explaining the observed abundances of CH_4, NH_3, H_2O, and SiH_4 are still lacking.

Outer Envelope Region: Photochemistry

The chemistry changes drastically when interstellar UV radiation can penetrate the more tenuous outer regions of the CSE, and photochemistry starts

to control molecular abundances. Neutral molecule plus radical reactions and neutral molecule plus ion ("ion-molecule") reactions are important for the production of many organic molecules in the outer CSE, particularly in C-rich objects (e.g., *4,52 58-63*).

Frequently employed tracers for photochemistry in CSE are CO, which photodissociates in the outer regions of the CSE, and CN and OH, which are photodissociation products of HCN and H_2O, respectively. Photodissociation of photospheric parent molecules (e.g., $H_2O + h\nu \rightarrow OH + H$; $C_2H_2 + h\nu \rightarrow C_2H + H$; $HCN + h\nu \rightarrow CN + H$) increases the radical abundances, and abundances of parent molecules start to decline. The distance in the CSE at which photodissociation begins is different for different parent molecules and reflects the distance where the CSE becomes transparent for the UV radiation to drive the photodissociation reaction.

Photoionizaton of neutral C to C^+ and C_2H_2 to $C_2H_2^+$ by UV photons and cosmic ray ionization of H_2 to H_3^+ are the major ion sources for subsequent ion molecule reactions and dissociative recombination reactions (*59*). So far only two ions (HCO^+, C_6H^-*(60)*) have been observed in IRC+10216. Ion-molecule reactions involving $C_2H_2^+$ can account for the abundances of several molecules produced in the outer CSE (e.g., C_nH, C_nS, C_3O, CH_3CN, HNC, C_nN, $C_3H_2HC_{2n+1}N$, etc.), but other reactions may also be required (*59-64*).

Neutral molecule plus radical reactions in the outer CSE are probably the major production channel of longer C-chain molecules such as $C_{2n}H$, and the cyanopolyynes ($HC_{2n+1}N$). For example, the reaction channel $C_{2n}H_2 + C_2H \rightarrow C_{2n+2}H_2 + H$ and subsequent photodissociation: $C_4H_2 + H \rightarrow C_4H + H$ can build up C_4H and C_6H from the parent molecule C_2H_2 (*62*).

Dust Grains from AGB Stars in Meteorites

Primitive (i.e., thermally unaltered) meteorites are now known to contain nm to micron-size grains with substantially different isotopic compositions in C, N, O, and Si than other solar system materials. The isotopic compositions link the majority of these grains to AGB stars (>95%) and supernovae. Because such grains must predate the formation of our solar system, they are collectively called "presolar grains". Detailed reviews about presolar grains are given in (*65,66*). The major known presolar minerals are refractory solids that condense at relatively high temperatures and are resistant to physical and chemical (laboratory) processing. Currently known presolar minerals include corundum (Al_2O_3), spinel ($MgAl_2O_4$), silicates of the pyroxene and olivine groups, graphite, diamond, and silicon carbide (SiC). Most of the oxide and silicate grains are ascribed to RG and O-rich AGB stars, and most of the SiC and graphite grains seem to come from C-rich AGB stars. Known minerals from

supernovae include graphite, SiC, and Si_3N_4 (sinoite); however, these grains are rare, although supernovae are thought to be major dust producers. The origin of presolar nano-diamonds is not well known, in part because individual grains cannot be analyzed.

Examples of rarer but larger presolar graphite grains with "cauliflower" and "onion" morphology are shown in Figure 5. Some of the micron-size graphite grains contain sub-grains of 10-100 nanometer-size carbides; either pure TiC or (Ti,Zr,Mo)C from AGB stars, or TiC and metallic particles of varying Fe-Ni content from supernovae. Often the refractory carbides are located in or near the center of graphite grains, which indicates that they formed first and acted as nucleation seeds for the graphite (*67*). The elemental compositions of presolar grains are used to determine their stellar sources and the environmental conditions in which the grains formed. For example, the measured trace element abundances in SiC grains from AGB stars are well understood to result from fractional equilibrium condensation close to the photospheres of the stars (*33*,*34*,*66*). The measured isotopic compositions of trace elements also provide sensitive tests to nucleosynthesis models (see reviews *65*,*66*).

AGB stars return ~0.3 solar masses per year to the interstellar medium (ISM) in our galaxy (*68*), of which C stars contribute about 10–50% (*14*,*30*). Thus, dust condensation in the circumstellar envelopes of C stars is a plausible source of the presolar C-bearing grains found in meteorites. Although carbonaceous dust is observed in CSEs, neither SiC nor carbon dust has yet been detected in the interstellar medium; instead, only silicate dust is detected (e.g., *40*). The reason for the apparently missing SiC in the ISM is still not clear. It has been suggested that SiC grains become coated with silicate mantles, and that such composite grains may prevent detection of the 11.3 μm SiC absorption feature (*69*). Such composite grains have not yet been discovered among presolar grains studied thus far. Still, if the theoretical predictions of grain processing in the ISM are correct, such grains should have been with those that traveled through the ISM from their parent stars to the molecular cloud from which the solar system formed.

Summary

Stars with initial masses of ~1-8 $M_\odot$ evolve into red giant stars and lose their outer atmospheres through stellar winds. The lost material creates huge circumstellar shells. The overall composition of a CSE is determined by the ongoing nucleosynthesis in the star. Most importantly, production and dredge-up of C in AGB stars changes the surface composition from oxygen rich (C/O<1 in M stars) to carbon-rich (C/O>1 in C stars). The C/O ratio determines the gas chemistry in the CSE and which condensates (e.g., silicates or carbides) appear.

The chemistry in the CSE depends on the distance from the star as temperatures and densities drop steeply with increasing distance. Equilibrium thermochemistry and condensation chemistry dominate in the photospheric and inner CSE regions (< 3-5 stellar radii). With increasing distance from the star, abundances become controlled by reaction kinetics. Abundances of important gases (CO, H_2O, C_2H_2, HCN, SiO…) become frozen-in. Gas-grain reactions are probably important to explain the relatively large abundances of CH_4, NH_3, SiH_4, H_2O that appear at low temperatures further from the central stars. Photochemistry produces many radicals and unsaturated gases in the outer CSE; e.g., C_nH (n=2-8), $HC_{2n+1}N$ (n=1-3).

Genuine star dust is preserved in meteorites. Most of the presolar grains comes from RG and from O-rich and C-rich AGB stars. Dust from supernovae and novae has also been found. Elemental, isotopic, and structural analyses of this star dust gives details on stellar nucleosynthesis and dust formation conditions in the circumstellar environments.

Acknowledgements

This work was supported in part by NASA grant NNG04GG13G. I thank Bruce Fegley, Jon Friedrich, Hans Olofsson, Laura Schaefer, and Lori Zaikowski for comments on the manuscript.

References

1. Iben, I. Renzini, A. *Annu. Rev. Astron. Astrophys*. **1983**, *21*, 271
2. Lafon, J.P.J; Berruyer, N. *Astron. Astrophys. Rev*. **1991**, *2*, 249
3. Clegg, R.E.S.; Stevens, I.R.; Meikle, W.P.S. Circumstellar media in the late stages of stellar evolution, Cambridge Univ. Press, **1996**, pp. 345
4. Glassgold, A.E. *Annu. Rev. Astron. Astrophys.* **1996**, *34*, 241
5. Habing, H.J. *Astron. Astrophys. Rev*. **1996**, *7*, 97
6. Bernatowicz, T.J.; Zinner, E. Astrophysical implications of the laboratory study of presolar materials, AIP Conf. Proc. 402, **1997**, pp.750
7. Busso, M.; Gallino, R.; Wasserburg, G. J. *Annu. Rev. Astron. Astrophys.* **1999**, *37*, 239
8. Lamers, H.J.G.L.M.; Cassinelli, J.P. Introduction to stellar winds, Cambridge Univ. Press, **1999**, pp. 438
9. LeBertre, T.; Lebre, A; Waelkens, C. (eds.) Asymptotic giant branch stars, IAU symposium no. 191, **1999**, Astronomical Soc. Pacific, pp. 632
10. Habing, H.J. Olofsson, H. (eds.) Asymptotic giant branch stars, Springer, Berlin, **2003**, pp. 559.

11. Lodders, K. *Astrophys. J.* **2003**, *591*, 1220
12. van Belle, G.T.; Dyck, H.M.; Thompson, R.R.; Benson, J.A.; Kannappan, S.J. *Astron. J.* **1997**, *114*, 2150.
13. Loup, C.; Forveille, T.; Omont, A.; Paul, J.F. *Astron. Astrophys. Suppl.* **1993**, *99*, 291
14. Schoier, F.L.; Olofsson, H. *Astron. Astrophys*. **2001**,368, 969
15. Winters, J.N.; LeBertre, T.; Jeong, K.S.; Nyman, L.A.; Epchtein, N. *Astron. Astrophys*. **2003**, *409*, 715
16. Gilman, R. C. *Astrophys. J.* **1972**, *178*, 423
17. Goldreich, P.; Scoville, N. *Astrophys. J.* **1976**, *205*, 144
18. Jones, T.T.; Ney, E.P; Stein, W.A. *Astrophys. J.* **1981**, *250*, 324
19. Gail, H.P.; Sedlmayr, E. *Astron. Astrophys*. **1987**, *177*, 186
20. Habing, H.J.; Tignon, J.; Tielens, A.G.G.M. *Astron. Astrophys*. **1994**, *286*, 523
21. Hoffmeister, C.; Richter, R.; Wenzel, W. Variable stars, Springer, Berlin, **1985**, pp. 328
22. Bowen, G.H. Astrophys. J. **1988**, *329*, 299
23. Fleischer, A.J.; Gauger, A.; Sedlmayr, E. Astron. Astrophys. **1992**, *266*, 321
24. Höfner, S. Feuchtinger, M.U.; Dorfi, E.A. Astron. Astrophys. **1995**, *297*, 815
25. Jorgensen, U.G.; Hron, J.; Loidl, R. Astron. Astrophys. **2000**, *356*, 253
26. Lambert, D. L.; Gustafsson, B.; Eriksson, K.; Hinkle, K. H. *Astrophys. J. Suppl.* **1986,** *62*, 373
27. Tsuji, T.; Ohnaka, K.; Aoki, W. *Astron. Astrophys.* **1997**, *320*, L1
28. Ohnaka, K.; Tsuji, T.; Aoki, W. *Astron. Astrophys.* **2000**, *353*, 528
29. Olofsson, H.; Bergman, P.; Eriksson, K.; Gustafsson, B. *Astron. Astrophys*. **1996**, *311*, 587
30. Guglielmo, F.; Epchtein, N.; LeBertre, T; et al. *Astron. Astrophys. Suppl. Ser*. **1993**, *99*, 31
31. Kwok, S. *Annu. Rev. Astron. Astrophys.* **1993**,*31*, 63
32. Tsuji, T. 1973, *Astron. Astrophys*. **1973**, *23*, 411
33. Lodders, K.; Fegley, B.; *Meteoritics* **1995**, *30*, 661
34. Lodders K, Fegley B.; *AIP Conf. Proc.* **1997**, *402*, 391
35. Ferrarotti, A.S.; Gail, H.P *Astron. Astrophys*. **2002**, *382*, 256
36. Smith; V.V.; Lambert, D.L. *Astrophys. J. Suppl.* **1990**, *72*, 387
37. Abia, C.; Dominguez, I; Gallino, R.; Busso, M.; Masera, S.; Straniero, O.; de Laverny, P.; Plez, B.; Isern, J. *Astrophys. J.* **2002**, *579*, 817
38. Bergeat, J.; Lefevre, J.; Kandel, R.; Lunel, M.; Sibille, F. *Astron. Astrophys*. **1976**, *52*, 245
39. Danchi, W. C.; Bester, M.; *Astrophys. Space Sci.* **1995**, *224*, 339
40. Molster, F.; Kemper, C. *Space Sci. Rev.* **2005**, *119*, 3

41. van der Veen, W.E.C.J.; Habing, H.J. *Astron. Astrophys.***1988**, *194*,125.
42. Hony, S.; Waters, L.B.F.M.; Tielens, A.G.G.M. *Astron. Astrophys.* **2002**, *390*, 533
43. Jimenez-Esteban, F.M.; Agudo-Merida, L.; Engels, D.; Garcia-Lario, P. *Astron. Astrophys.* **2005**,*431*, 779
44. Keady, J.J.; Ridgway, S.T.; *Astrophys. J.* **1993**, *406*, 199
45. Bieging, H.H.; Tafalla, M.; *Astron. J.* **1993**, *105*, 576
46. Olofsson, H.; Eriksson, K.; Gustafsson, B.; Carlstrom, U.; *Astrophys. J. Suppl.* **1993**, *87*, 267
47. Olofsson, H.; Eriksson, K.; Gustafsson, B.; Carlstrom, U.; *Astrophys. J. Suppl.* **1993**, *87*, 305
48. Bieging, J.H.; Shaked, S.; Gensheimer, P.D. *Astrophys. J*. **2000**, *543*, 897
49. Lindqvist, M.; Schoier, F.L.; Lucas, R.; Olofsson, H.; *Astron. Astrophys.* **2000**, *361*, 1036
50. Woods, P.P.; Schoier, F.L.; Nyman, L.A.; Olofsson, H.; *Astron. Astrophys.* **2003**, *402*, 617
51. Gonzales Delagado, D.; Olofsson, H.; Kerschbaum, F.; Schöier, F.L.; Lindqvist, M.; Groenewegen, M.A.T. *Astron. Astrophys.* **2003**, *411*, 123
52. Lafont, S.; Lucas, R.; Omont, A. *Astron. Astrophys.***1982**, *106*, 201
53. Prinn, R.; Fegley, B.; in Origin and evolution of planetary and satellite atmospheres, Univ. Arizona Press, 1989, pp. 89
54. Lodders, K.; Fegley, B. *Icarus* **2002**, *155*, 393
55. Monnier, J.D.; Danchi, W.C.; Hale, D.S.; Tuthill, P.G.; Townes, C.H. *Astrophys. J.* **2000**, *543*, 868
56. Hasegawa, T.I.; Kwok, S.; Koning, N.; Volk, K.; Justtanont, K.; Olofsson, H.; Schöier, F.L.; Sandqvist, A.; Hjalmarson, A.; Olberg, M; Winnberg, A.; Nyman, L.A.; Frisk, U. Astrophys. J. **2006**, *637*, 791
57. Menten, K.M.; Alcolea, J. *Astrophys. J.* **1995**, *448*, 416
58. Huggins, P.J.; Glassgold, A.E. *Astron. J.* **1982**, *87*, 1828
59. Glassgold, A.E.; Lucas, R.; Omont, A. *Astron. Astrophys*. **1986**, *157*, 35
60. McCarthy, M.C.; Gottlieb, C.A.; Gupta, H.; Thaddeus, P. *Astrophys. J.* **2006**, *652*, L141
61. Nejad, L.A.M.; Millar, T.J. *Astron. Astrophys.* **1987**, *182*, 279
62. Howe, D.A.; Millar, T.J.; *Mon. Not. R. Astr. Soc*, **1990**, *244*, 444
63. Millar, T.J.; Herbst, E. *Astron. Astrophys,*. **1994**, *288*, 561
64. Doty, S.D.; Leung, C.M. *Astrophys. J*. **1998**, *502*, 898
65. Zinner, E. in Treatise on Geochemistry 1, Elsevier, Oxford, 2004, pp. 17
66. Lodders, K.; Amari, S. *Chem. Erde* **2005**, *65*, 93
67. Bernatowicz, T.J.; Cowsik, R.; Gibbons, P.C.; Lodders, K.; Fegley, B.; Amari, S.; Lewis, R.S. *Astrophys. J.* **1996**, *472*, 760
68. Knapp, G.R.; Morris, M. *Astrophys. J.* **1985**, *292*, 640
69. Ossenkopf, V.; Henning, T.; Mathis, J.S. *Astron. Astrophys*. **1992**, *261*, 567

Figure Captions

Figure 5. Scanning electron microscopic photographs of 2 circumstellar graphite grains (top) and a presolar SiC grain (bottom) isolated from meteorites. Photos courtesy of Sachiko Amari.

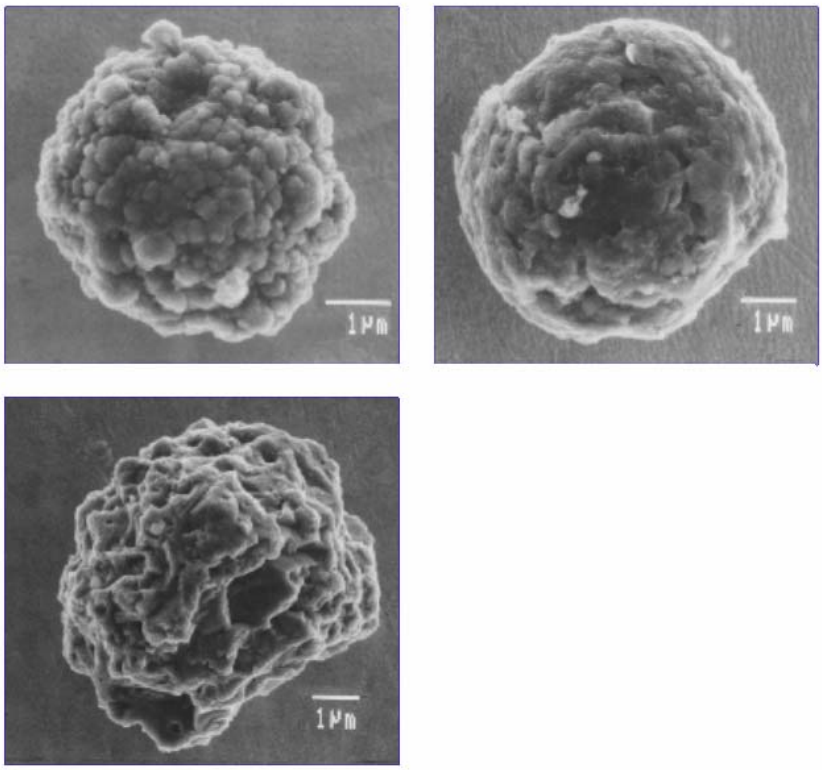
1µm
1µm
1µm